Photochemical Studies of the Alkylammoniun Molybdates. Part 5.[1] Photolysis in Weak Acid Solutions

By **Toshihiro Yamase,* Ryoichi Sasaki,** and **Tsuneo Ikawa,** Research Laboratory of Resources Utilization, Tokyo Institute of Technology, 4259 Nagatsuta, Midori-ku, Yokohama 227, Japan

Solution photolysis of hexakis(isopropylammonium) heptamolybdate(VI) trihydrate, $[NH_3Pr^i]_6[Mo_7O_{24}]\cdot 3H_2O$ (1), at pH 5.4 leads to reduction to Mo^V with involvement of hydroxy-radicals, followed by decomposition to yellow and blue species. Propylene and acetone were detected as oxidation products but quantum yields for their formation were much lower than that for Mo^V formation. The irradiated single-crystal e.s.r. spectra revealed the formation of $Mo^VO_5(OH)$ in a MoO_6 octahedral site, which corresponded to the primary event in the solution photolysis. E.s.r. and Raman spectroscopy and flash photolysis were employed to elucidate the mechanism of these reactions.

We recently reported an example of photogalvanic behaviour based on the photoreduction of Mo^{VI} to Mo^V for an aqueous solution of an alkylammonium polymolybdate and its application to water decomposition.[2,3] Several generalisations with regard to the photochemical properties of the molybdates in the solid state and as aqueous solutions have been described.[1-5] The purpose of the work reported in this paper is to investigate the mechanism of the solution photolysis of hexakis(isopropylammonium) heptamolybdate trihydrate, $[NH_3Pr^i]_6[Mo_7O_{24}]\cdot 3H_2O$ (1), as the molybdate. A mechanism for the solution photolysis is proposed which is consistent with the results of quantum yield, e.s.r. spectra for solution and solid states, Raman spectra, and flash photolysis.

EXPERIMENTAL

All chemicals were of Tokyo Kasei G.R. or analytical grade and were used without further purification. Hexakis(isopropylammonium) heptamolybdate trihydrate (1) was prepared and recrystallised following our procedure [5] and its structure (a = 23.904, b = 10.504, c = 20.652 Å, β = 115.4°, space group $P2/n$, Z = 4, R = 0.053) was determined by a single-crystal X-ray diffraction study [6] (Found: C, 13.35; H, 4.25; Mo, 44.9; N, 5.15. Calc. for $[NH_3Pr^i]_6[Mo_7O_{24}]\cdot 3H_2O$: C, 14.7; H, 4.50; Mo, 45.7; N, 4.35%).

2-Methyl-2-nitrosopropane (menp) and N-benzylidene-t-butylamine N-oxide (bbao), used for the e.s.r. spin-trapping techniques,[7] were prepared as described by Emmons.[8] Solutions of $[NH_3Pr^i][ClO_4]$ (pH 5—6) were prepared by mixing NH_2Pr^i with $HClO_4$ aqueous solutions. Unless otherwise specified, all measurements were carried out at room temperature. The evacuation of solutions was carried out by several freeze-pump-thaw cycles to 10^{-4} Torr.†

Continuous-irradiation experiments were carried out using a 500-W super-high-pressure mercury lamp in conjunction with filters.[5] Chemical actinometry was carried out using the potassium ferrioxalate system.[9] A gas chromatographic method (Shimazu GC-4C chromatograph with a Porapak T column) and mass spectrometry were employed for analysis of propylene over the aqueous solution. Propylene concentration in aqueous solutions was calculated by assuming Bunsen's absorption coefficient of 0.11 (at 23 °C) which was the value for ethylene. Analysis of acetone in the photolyte was made by colorimetry of the monohydrazone formed with oxalyldihydrazine at pH 10.[10] Absorbance of the aqueous solutions was measured on a Hitachi 624 spectrophotometer. The ^1H n.m.r. data were obtained from saturated solutions (0.51 mol dm^{-3}) of compound (1) in D_2O using a JEOL-PS-100 spectrometer with $SiMe_4$ as the external standard.

X-Band e.s.r. spectra were recorded on a Varian E12 spectrometer. For quantitative e.s.r. measurements, the derivative signal due to Mo^V in u.v.-irradiated powder of compound (1) was doubly integrated and compared with a double-integrated signal for the diphenylpicrylhydrazyl (dpph) standard.[5] The single-crystal e.s.r. spectra were recorded as previously described.[1] The crystals were mounted such that the magnetic field could be orientated in the a^*b, bc, and ca^* crystallographic planes.

Raman spectra of the aqueous solutions were measured using the combination of a JEOL Raman spectrophotometer and a Coherent Radiation CR4 Ar^+ laser (514.5 nm) or rhodamine 6G dye laser (598.8 nm) pumped with the Ar^+ laser. The flash-photolysis experiment was carried out using a Xenon Corp. model 720 flash-photolysis apparatus. A lifetime of 100 μs was measured for the flash pulse under the experimental conditions. The electrical signal was measured on a Sony–Tektronix 475 oscilloscope.

RESULTS

Photoproducts and Quantum Yield.—Aqueous solutions of (1) showed an absorption maximum at 205 nm (ε 1.56 × 10^2 m^2 mol^{-1}) with shoulders at about 230 nm (ε 86) and 285 nm (ε 25 m^2 mol^{-1}) and much weaker absorptions at wavelengths between 310 and 380 nm (ε_{313} 9.7 and ε_{365} 4.1 m^2 mol^{-1}).[2] The pH of all the solutions was 5.4 before and after irradiation with light of wavelength 313 or 365 nm.

Steady-state photolysis of a deaerated solution of (1) yields blue ($\lambda_{max.}$ 730, $\lambda_{(sh)}$ 620 nm) and yellow species as final photoproducts. The concentration ratio of the blue to yellow species increases with increasing initial concentration of (1) as shown in Figure 1(*a*). The photolysis of the solution containing a low concentration ($\leqslant$2.7 mmol dm^{-3}) of (1) results in the development of a yellow colour due to an absorption with a long shoulder sloping into the visible region. On addition of (1) (or $[NH_4]_6[Mo_7O_{24}]\cdot 4H_2O$) the yellow solution turns blue and the blue colour deepens with increasing concentration of additional $[Mo_7O_{24}]^{6-}$, as shown in Figure 1(*b*) where the absorbance at 730 nm is plotted against the additional $[Mo_7O_{24}]^{6-}$ concentration.

† Throughout this paper: 1 Torr = (101 325/760) Pa; 1 G = 10^{-4} T; 1 cal = 4.184 J; 1 E (Einstein) = 1 mol of photons.

The results indicate that the blue species arises from a reaction between $[Mo_7O_{24}]^{6-}$ and the yellow species. The effect of the initial concentration of (1) on the concentration ratio of the blue to yellow species in the photolyte follows the same pattern as in the aqueous solution of the u.v.-irradiated powder of compound (1) for the first 10% of the photolysis reaction.[4,5] The photometric determination of Mo^V in the deaerated solution was therefore carried out using

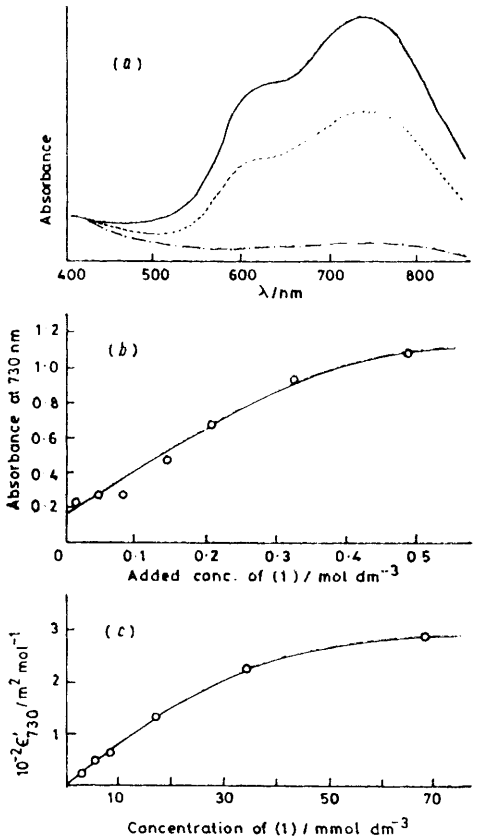

FIGURE 1 Effect of the concentration of $[NH_3Pr^i]_6[Mo_7O_{24}]$ (1) on the absorption spectrum obtained after photolysis (365 nm). (*a*) Initial concentration of (1): 27.2 mmol dm^{-3} (——), 13.6 mmol dm^{-3} (– – – –), 2.7 mmol dm^{-3} (— · —). The curves (taken from the first 10% of the photolysis) are normalised to the absorbance at 400 nm for comparison. (*b*) Mixing of (1) with the photolyte [initial concentration of (1) = 1.7 mmol dm^{-3}] containing 5.5×10^{-4} mol dm^{-3} Mo^V. Mixing of $[NH_4]_6[Mo_7O_{24}]\cdot 4H_2O$ with the solution gives the same effect as for (1). Absorbance at 730 nm indicates the value for an optical path length of 1 cm. (*c*) Photometry of Mo^V in the deaerated photolyte (within the first 10% of the photolysis) as a function of the initial concentration of (1) at 23 °C

ε'_{730} values which were obtained from Beer's law [*i.e.* the relationship between the Mo^V concentration in the u.v.-irradiated powder of (1) and the absorbance of the solution at 730 nm as a function of the initial concentration of (1), see Figure 1(*c*)].

The effects of the initial concentration of (1), the light intensity, and $[NH_3Pr^i][ClO_4]$ concentration on quantum yields (ϕ) of Mo^V formation for the deaerated solutions are summarised in Table 1, where ϕ increases slightly with increasing concentration of (1) and decreasing light intensity and increases considerably with increasing $[NH_3Pr^i][ClO_4]$ concentration. No significant difference in ϕ between 313 nm and 365 nm photolysis suggests that the photolysis is wavelength independent. The quantum yield was little affected by the variation of ionic strength with $Na[ClO_4]$, when other parameters were kept constant. During the continued photolysis of the solution, propylene and acetone were detected. The formation of acetone was also evidenced by the ^1H n.m.r. investigation. The prolonged irradiation (about 10 h) of the saturated solution of (1) in D_2O resulted in the appearance of a single line due to acetone with a chemical shift of 2.48 p.p.m. relative to $SiMe_4$. Quantum yields of propylene and acetone formations were about 8×10^{-3} and 3×10^{-4} respectively for 313 nm photolysis (1.1×10^{-4} E dm^{-3} min^{-1}) of a deaerated solution containing 13.6 mmol dm^{-3} of (1). These values are much lower than the quantum yield (0.28) of Mo^V formation, indicating that there is little destruction of NH_3Pr^i cations

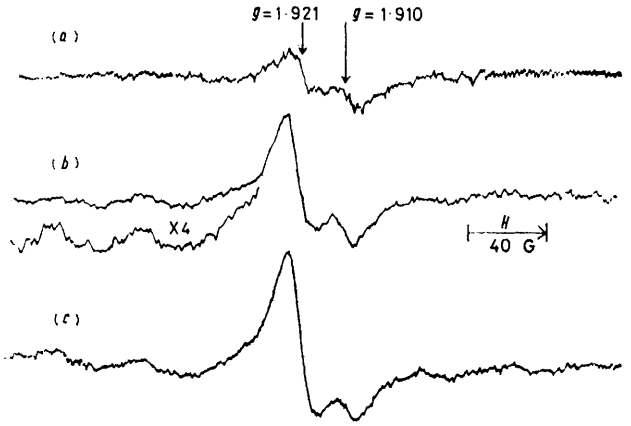

FIGURE 2 E.s.r. spectra for deaerated photolysed solutions: (*a*) 2.7 mmol dm^{-3} (1) at 0—65 °C, (*b*) 27.2 mmol dm^{-3} (1) at 23 °C, (*c*) 27.2 mmol dm^{-3} (1) at about 56 °C

in the photoreaction. Solutions of $[NH_3Pr^i][ClO_4]$ (pH 5—6) did not give any significant yield of propylene and acetone under irradiation with 313-nm light in the absence of the molybdate.

Electron Spin Resonance.—Two paramagnetic species are found for the deaerated photolyte at pH 5.4 and the intensity ratio of their e.s.r. signals depends on the initial concentration of (1), as shown in Figure 2. At low concentration ($\leqslant 2.7$ mmol dm^{-3}) of (1) two weak signals at $g = 1.921$ and 1.910 were detected. At high concentration of (1) a well defined signal at $g = 1.921$ developed with six weak satellite lines due to ^{95}Mo and ^{97}Mo (nuclear spin $I = \frac{5}{2}$, natural abundance 25%). The hyperfine splitting constant was 51 G (4.6×10^{-3} cm^{-1}). The intensity ratio of the signal at $g = 1.921$ to that at $g = 1.910$ increased reversibly with increasing temperature, with an accompanying fading of the blue colour (blue⇌greenish yellow); the heat of reaction (ΔH_r) was about 15 kcal mol^{-1}, as shown previously.[5] In conjunction with the results (Figure 1) of the dependence of the initial concentration of (1) on the ratio of concentrations of the blue to the yellow species in the photolyte, these results indicate that the yellow form must consist of at least two different paramagnetic species, one ($g = 1.921$) of which is involved in the thermochromism with the blue species with ΔH_r *ca.* 15 kcal mol^{-1}.

The fact that dissolution of crystals of the irradiated solid in water [4,5] leads to the same species as the solution photo-

TABLE 1

Quantum yield (ϕ) for Mo^V formation * for deaerated solutions

Initial concentration of (1)/mmol dm^{-3}	Incident light intensity/ 10^{-5} E dm^{-3} min^{-1}	$[NH_3Pr^i][ClO_4]$ concentration/ mmol dm^{-3}	$Na[ClO_4]$ concentration/ mol dm^{-3}	ϕ_{313}	ϕ_{365}
136	4.5 (313 nm), 19 (365 nm)				0.55
29.2				0.48	0.48
27.2				0.48	0.51
19.0				0.49	
13.6				0.32	
2.7				0.28	
27.2	66 (365 nm)				0.47
	44				0.43
	28				0.50
	13				0.58
	4.7				0.67
	2.1				0.67
	0.9				0.68
				0.28	
		4.5		0.29	
		18.0		0.34	
13.6	11 (313 nm)	45.0		0.39	
		89.9		0.57	
		179.9		0.80	
		359.7		0.97	
		899.4		1.10	
			0.05		0.53
27.2	19 (365 nm)		0.5		0.42
			1.5		0.41

* ϕ_{313} and ϕ_{365} indicate the quantum yields obtained by using the exciting light of 313 nm and 365 nm, respectively. Data are extracted within the first 5% of the photolysis.

lysis, and that the predominant molybdate anion at pH 5.4 is $[Mo_7O_{24}]^{6-}$,[11] suggestt that the photochemical process in the solid state represents a primary event in the solution photolysis. Bearing this in mind, e.s.r. spectra of the irradiated single crystal of (1) were measured. A typical e.s.r. spectrum is shown in Figure 3, where there are two sets of lines arising from two magnetically inequivalent Mo^V centres (A and B). Each of the Mo^V centres exhibits a main line arising from the non-magnetic ^{96}Mo nucleus, split into two hyperfine lines (1 : 1) owing to superhyperfine interaction with a hydrogen atom, with six weak satellite lines due to ^{95}Mo and ^{97}Mo. Each of the hyperfine lines due to ^{95}Mo and ^{97}Mo is resolved into two superhyperfine lines at several orientations of the magnetic field. The occurrence of a six-line hyperfine structure is characteristic of an unpaired electron localised on one molybdenum atom only. Furthermore, the lines are narrow and no exchange broadening is observed. From these results it is inferred that one molecule of (1) contains at best one Mo^V centre. This is in agreement with the crystal structure which shows a total of four molecules per unit cell (two sets of two equivalent molecules related by a centre of inversion in the unit cell). The e.s.r. results were fitted to the Hamiltonian (i). In two magnetically inequivalent Mo^V centres per unit cell the final e.s.r. parameters were obtained by an iterative least-squares procedure utilising exact diagonalisations of the Hamiltonian matrix according to the previous method.[1] The g, $|A_{Mo}|$, and $|A_H|$ tensors for the two Mo^V centres (A and B) are shown in Table 2. The Mo^V A and B centres differ only in the orientation of the principal molecular g values: g_1 = 1.899 (1.898 for B), g_2 = 1.935 (1.936),

TABLE 2

Electron spin resonance parameters for Mo^V(A) and (B) centres

Principal values Mo^V (A) centre		Direction cosines with respect to (a^*)	(b)	(c)
g_1	1.899	0.726 0	−0.687 6	0.010 5
g_2	1.935	−0.618 2	−0.717 0	0.147 9
g_3	1.924	0.094 1	0.114 5	0.989 0
g_0 [a]	1.919			
$\lvert A_{Mo(1)}\rvert$	7.45	0.935 8	−0.327 8	0.129 8
$\lvert A_{Mo(2)}\rvert$	3.07	−0.351 5	−0.839 6	0.414 1
$\lvert A_{Mo(3)}\rvert$	3.40	0.026 8	0.433 1	0.900 9
$\lvert A_{Mo(0)}\rvert$	4.64			
$\lvert A_{H(1)}\rvert$	8.63	0.840 8	0.258 6	−0.475 7
$\lvert A_{H(2)}\rvert$	6.36	0.309 3	−0.950 5	0.029 9
$\lvert A_{H(3)}\rvert$	11.85	0.444 4	0.172 3	0.879 1
$\lvert A_{H(0)}\rvert$	8.95			
Mo^V (B) centre				
g_1	1.898	0.800 2	0.599 4	−0.018 0
g_2	1.936	0.558 6	−0.756 0	−0.341 3
g_3	1.922	0.218 1	−0.263 0	0.939 8
g_0 [a]	1.919			
$\lvert A_{Mo(1)}\rvert$	7.47	0.960 8	0.234 4	0.147 7
$\lvert A_{Mo(2)}\rvert$	3.71	0.080 1	−0.745 4	0.661 7
$\lvert A_{Mo(3)}\rvert$	2.85	−0.265 2	0.624 0	0.735 0
$\lvert A_{Mo(0)}\rvert$	4.58			
$\lvert A_{H(1)}\rvert$	9.39	0.755 6	−0.532 7	−0.381 2
$\lvert A_{H(2)}\rvert$	5.98	−0.507 1	−0.844 7	0.174 4
$\lvert A_{H(3)}\rvert$	11.58	0.414 7	−0.061 5	0.907 9
$\lvert A_{H(0)}\rvert$	9.98			

[a] $g_0 = (g_1 + g_2 + g_3)/3$. [b] $|A_{Mo}|$: units in 10^{-3} cm^{-1}, $|A_{Mo(0)}| = (|A_{Mo(1)}| + |A_{Mo(2)}| + |A_{Mo(3)}|)/3$. [c] $|A_H|$: units in 10^{-4} cm^{-1}, $|A_{H(0)}| = (|A_{H(1)}| + |A_{H(2)}| + |A_{H(3)}|)/3$.

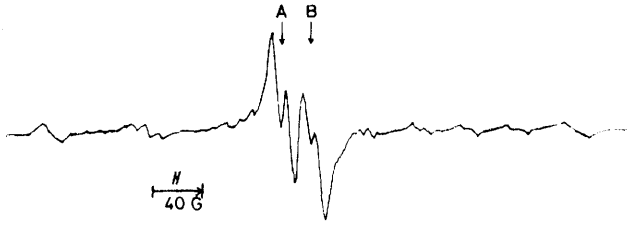

FIGURE 3 E.s.r. spectrum of an irradiated single crystal, with H_0 in the a^*b plane making an angle of 7° with the a^* axis

$$\mathcal{H} = \beta H g S + I_{Mo} A_{Mo} S + I_H A_H S \qquad \text{(i)}$$

and $g_3 = 1.924$ (1.922), with respect to the crystallographic axes. The g_0, $|A_{Mo(0)}|$, and $|A_{H(0)}|$ values of the Mo^V(A) centre are fairly close to those of the Mo^V(B) centre, as shown in Table 2. This suggests that there is structurally no significant difference between the two magnetically inequivalent Mo^V centres. From the correlation with *X*-ray crystal-structure data,[6] the paramagnetic centre can be associated with $Mo^VO_5(OH)$, resulting from the u.v.-induced proton transfer from a NH_3Pr^i cation (not from water in the lattice) to an O atom in an MoO_6 octahedral site. A similar conclusion has been described for the irradiated $[NH_3Pr^i]_6[H_2Mo_8O_{28}]\cdot 2H_2O$ single crystal.[1,12]

In order to detect short-lived free radicals in the solution photolysis, spin-trapping techniques using menp or bbao as spin traps were applied. Photolysis (5—15 s, $\lambda = 365$ nm) of the deaerated solution containing 68 mmol dm^{-3} (1) and 0.1 mol dm^{-3} menp gave an e.s.r. spectrum comprising a triplet of doublets with $a_N = 16.1$, $a_H = 4.0$ G at pH 5.4,

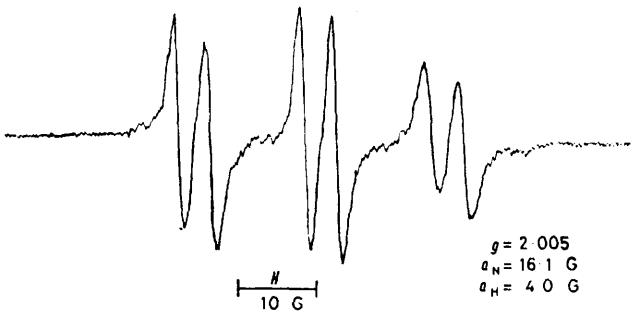

FIGURE 4 E.s.r. spectrum ($g = 2.005$, $a_H = 4.0$ G, $a_N = 16.1$ G) of nitroxide radical formed in the photolysis of (1) (initial concentration = 27.2 mmol dm^{-3}) in the presence of menp (2.3 mmol dm^{-3})

which can be assigned to menp spin-adduct radicals of hydroxy (·OH) or perhydroxy (HO_2·) radicals (Figure 4).* In the absence of (1) no such signals were observed. Solutions of (1) with 0.1 mol dm^{-3} bbao gave after 5 s irradiation a spectrum of a triplet of doublets with $a_N = 16.3$, $a_H = 3.8$ G. In studies of bbao spin adducts of ·OH and HO_2· it has been reported that both a_N and a_H values vary with different sources of these radicals and that approximately linear relationships ($a_H = 0.604\ a_N - 6.53$ and $a_H = 1.26\ a_N - 15.7$ G) between a_H and a_N are observed for ·OH and HO_2· respectively.[13] If this relationship is valid for the present system, the bbao spin adduct produced is assumed to be the ·OH adduct.†

Raman Spectra and Flash Photolysis.—Raman spectra of solutions before and after u.v. (313 nm light) irradiation are shown in Figure 5, where the spectrum of $Na_2[MoO_4]$ solution is added for comparison. Comparison of the Raman spectra [Figure 5(*a*) and (*b*)] measured with laser light (514.5 nm) scattering indicates that the photolysis leads to an increase in intensities at 310 and 898 cm^{-1} and a shift of the Mo=O stretching mode (938 cm^{-1}) in the octahedral MoO_6 unit to 945 cm^{-1}.[14] The spectrum [Figure 5(*c*)] measured with 598.8-nm dye laser excitation differs from that [Figure 5(*b*)] using laser light of 514.5 nm, suggesting that Figure 5(*c*) shows the resonance Raman spectrum for the blue species in the photolyte. The interesting feature in this spectrum is an appearance of new bands at 315, 335, and 965 cm^{-1}.

Flash photolysis of the deaerated solution was carried out. Two intermediates are formed by photoexcitation of (1), as shown in Figure 6. The first intermediate, I, with its broad absorption at the near-u.v.–visible range was produced during the lifetime of the flash. These absorptions

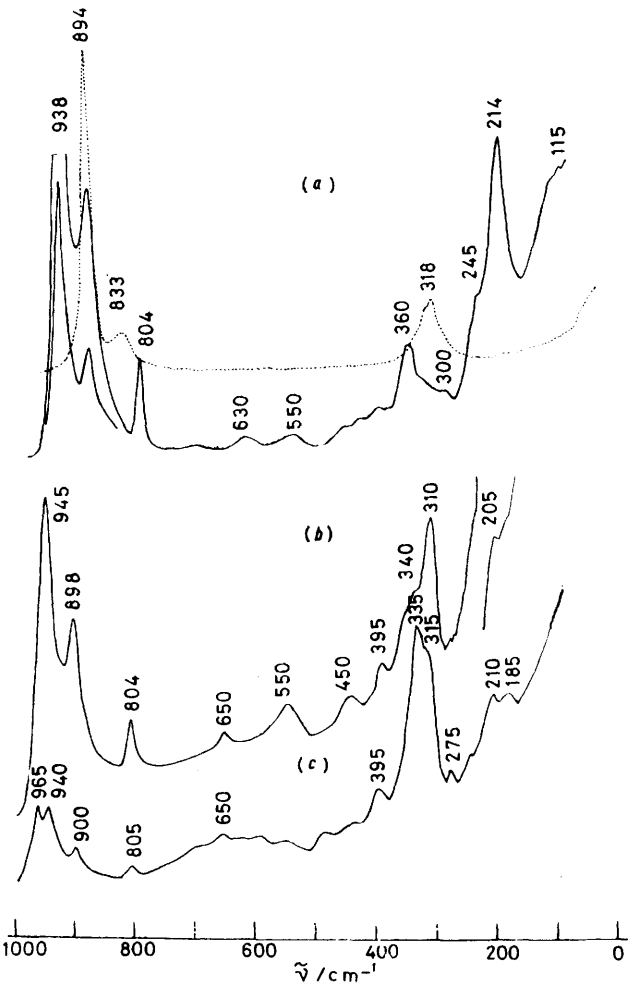

FIGURE 5 Raman spectra of deaerated solutions [initial concentration of (1) = 54.4 mmol dm^{-3}]. (*a*) Before photolysis, 514.5 nm laser-light scattering; (*b*) photolyte containing about 3 mmol dm^{-3} Mo^V, 514.5 nm laser-light scattering; (*c*) same solution as (*b*), 598.8 nm dye-laser excitation. Spectrum of $Na_2[MoO_4]$ solution (0.1 mol dm^{-3}) represented by (· · · ·)

disappeared by a transformation to the second intermediate, II, exhibiting $\lambda_{max.} = 500$ nm, with a first-order rate. The value of the decay rate constant, $(8 \pm 1) \times 10^3$ s^{-1}, was almost unchanged on variation of the concentration of (1) ($\leqslant 30$ mmol dm^{-3}), when the decay of these absorptions was followed at 450 nm. The same value was obtained for the formation of II followed at 700 nm. Under high concentrations ($\geqslant 10$ mmol dm^{-3}) of (1), intermediate II transformed very slowly by means of a pseudo-first-order reaction into the blue species which was the same species as under the steady-state irradiation [see Figure 1(*a*)]. A rate

* An irradiated solution of $[NH_2Me_2]_2[Mo_3O_{10}]\cdot H_2O$, whose crystal structure has not yet been determined, gave similar e.s.r. signals for an menp spin adduct at pH 4.3, showing ' 3 × 2 ' line structure ($a_H = 2.5$, $a_N = 15.4$ G).

† The photolysis of aqueous 30% H_2O_2 and bbao gave a bbao spin adduct of ·OH with $a_H = 3.1$ and $a_N = 15.7$ G.

constant [$(1.5 \pm 0.5) \times 10^{-2}$ s^{-1}] was obtained for such a decay followed at 500 nm. At low concentration ($\leqslant 10$ mmol dm^{-3}) of (1), low absorbance for the spectrum of II resulted in a difficulty in measuring the fate of II.

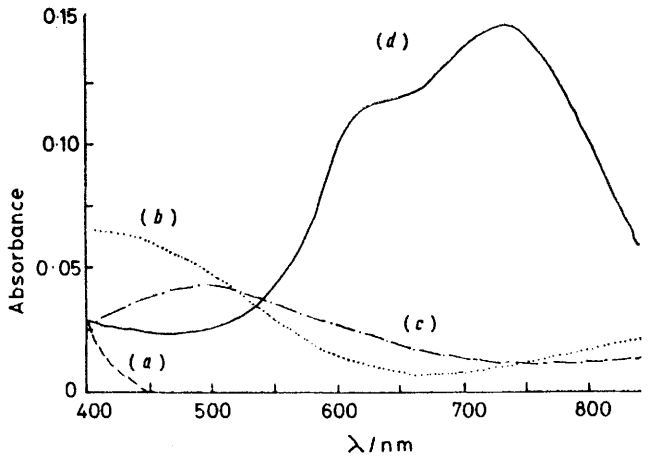

FIGURE 6 Transient electronic spectrum obtained in flash photolysis (250-J pulse) of deaerated solutions of (1) (27.2 mmol dm^{-3}). Curves are obtained at the following reaction times: (*a*) 0 ms, (*b*) 0.4 ms, (*c*) 1 ms, (*d*) 10 min; (*b*) and (*c*) correspond to intermediates I and II respectively

DISCUSSION

Although details of the *X*-ray crystal-structure data will be given elsewhere,[6] the $[Mo_7O_{24}]^{6-}$ anion of (1) consists of seven MoO_6 octahedra condensed by edge sharing and the Mo–O distances and O–Mo–O angles in these octahedra are in fair agreement with the corresponding ones found in the octahedra of $[NH_4]_6[Mo_7O_{24}]$ [15] and $[NH_3Pr^i]_6[H_2Mo_8O_{28}]$.[12] The mode of the solid-state photoreaction which corresponds to the primary process for the solution photolysis can be proposed as follows in reaction (1) showing a photoreducible

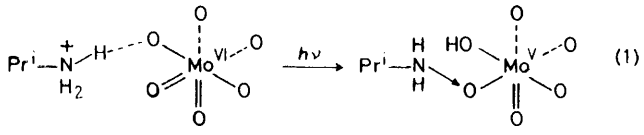

(1)

(i)

MoO_6 site (the Mo^{VI} atom is surrounded by a distorted octahedral set of six oxygen atoms, two of which are of *cis* terminal doubly bonded dioxo-groups and four are bridging). Photoreduction of Mo^{VI} to Mo^{V} may proceed *via* u.v.-induced charge transfer in the terminal Mo=O bond with an accompanying transfer of a hydrogen-bonding proton from the isopropylammonium nitrogen atom to a bridging oxygen atom, followed by an interaction of the non-bonding electrons of the amino-nitrogen with the terminal oxo-group leading to a charge-transfer complex (i), as was discussed previously.[1] In solution, structure (i) must undergo attack of a solvent water molecule to give rise to the formation of hydroxy-radicals [reaction (2)] which presumably form H_2O_2. Since NH_2Pr^i is a strong base in the system, it must be protonated just as it is formed. As a result, the overall reaction scheme for the initial step in solution is given by equation (3). The spin-trapping results provide clear

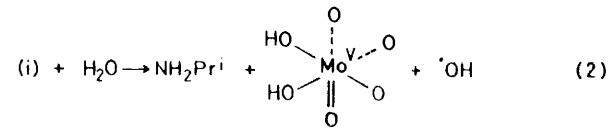

(2)

(ii)

evidence for the formation of ·OH and HO_2· (probably formed by oxidation of H_2O_2, $H_2O_2 \longrightarrow HO_2\cdot + H^+ + e^-$; or by a reaction between H_2O_2 and ·OH,

$$[NH_3Pr^i]_6[Mo_7O_{24}] + H_2O \xrightarrow{h\nu} [NH_3Pr^i]_6[Mo_7O_{23}(OH)] + \cdot OH \quad (3)$$

$H_2O_2 + \cdot OH \longrightarrow HO_2\cdot + H_2O$),[16] supporting the above reaction scheme. Table 1 shows that ϕ increases with an increase in $[NH_3Pr^i]^+$ concentration when the concentration of (1) was kept constant. This provides additional support to reactions (1)—(3), since the formation of complex (i) in solution would be facilitated by an increase in $[NH_3Pr^i]^+$ concentration.

If a charge-transfer complex mechanism for the initial step is assumed, a polar solvent water molecule may increase the extent of the charge separation in complex (i) [equation (4)]. This is represented in the redox

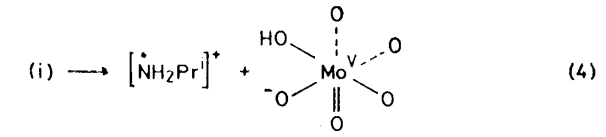

(4)

reaction (5) with the readily reducing NH_2Pr^i ligand promoting a quenching process of ·OH which is produced by reactions (2) or (3).

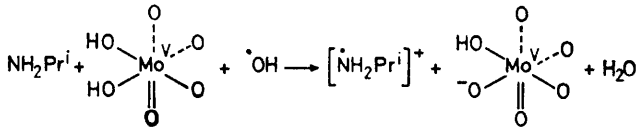

(5)

The electrochemical oxidation of a primary aliphatic amine has been examined and a dual mechanism has been suggested for the pathways to the amino-cation radical. One is the decomposition to a carbonium ion and amido-radical; the other is the loss of an α-proton to leave the neutral α-amino-radical.[17] The formation of propylene

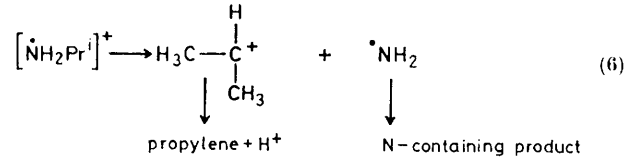

(6)

and acetone as minor photoproducts from $[NH_2Pr^i]^+$ can be accounted for by these two pathways, as shown in reactions (6) and (7). The formation of propylene and

acetone, therefore, supports the occurrence of reaction (4) or (5) and the involvement of ·OH in the photolysis. Analysis of gaseous content over the photolyte by mass

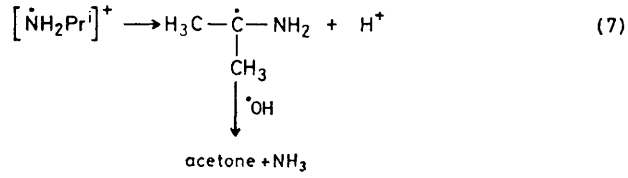

(7)

spectrometry gave no evidence of hydrazine which might be expected to be degraded to nitrogen gas. Reaction (8), which causes a recovery of $[NH_3Pr^i]^+$ and an increase in ·OH yield, may be considered. However, the poten-

$$[\dot{N}H_2Pr^i]^+ + H_2O \longrightarrow [NH_3Pr^i]^+ + \cdot OH \quad (8)$$

tial [2.5 V *vs.* n.h.e. (normal hydrogen electrode) at pH 5.4] for oxidation of H_2O to ·OH is more positive than that for the oxidation of NH_2Pr^i (*ca.* 1.6 V *vs.* n.h.e.),[16,18] so that we can exclude the possibility of reaction (8) corresponding to the reverse process of reaction (5).

Reaction (3) would involve formation of significant amounts of ·OH, considering the fact that the photoreduction to Mo^V occurred efficiently (see Table 1). Back reaction between the photoreduction molybdate and ·OH was assumed to be depressed under high concentration ($\geqslant$2.7 mmol dm^{-3}) of complex (1), since ϕ decreased very slightly with increasing light intensity and with decreasing concentration of (1), as shown in Table 1. There was no detection of H_2O_2, O_2, or diperoxoheptamolybdate [19] in significant quantities, although we could detect ·OH and HO_2· as intermediates in the photolysis. Judging from the fact that the quantum yield of Mo^V formation is more than 30 times higher than for the formation of propylene or acetone resulting from reaction (5), ·OH appears to react rapidly with $[Mo_7O_{24}]^{6-}$ to yield highly condensed molybdate. From the above results, however, further speculation of the fates of ·OH is inappropriate.

It must be noted that the standard redox potential, $E^\ominus(Mo^{VI}\text{–}Mo^V)$, for the electrochemically active species, which can be photochemically produced in solution, exhibited an approximately linear pH dependence with a slope of about −59 mV/pH.[3] This indicates that the anode reaction of the electrochemically active species is given by a protonation–deprotonation process [equation (9)]. In connection with the observation of a $Mo^VO_5(OH)$

$$Mo^V\text{–}OH \longrightarrow Mo^{VI}{=}O + H^+ + e^- \quad (9)$$

site in the irradiated single crystal, therefore, it is reasonable to assume that the co-ordination of the hydroxide to the paramagnetic Mo^V atom is also maintained in solution. No indication of a ^1H superhyperfine signal in the solution e.s.r. spectra (Figure 2) would be expected because of a line broadening due to two anisotropies of g and ^{95}Mo and ^{97}Mo hyperfine tensors. Values of $g = 1.921$ and $a_{Mo} = 51$ G (4.6×10^{-3} cm^{-1}) for one of the two stable paramagnetic species in the photolyte are in good agreement with the averages [g_0 and $|A_{Mo(0)}|$ in Table 2] of corresponding principal values measured from the irradiated single-crystal e.s.r. spectra. This result suggests that the species having $g = 1.921$ in the photolyte possesses the same structure as the octahedral Mo^V centre in $[Mo_7O_{23}(OH)]^{6-}$ for the single crystal. The presence of another paramagnetic species having $g = 1.910$ in the photolyte implies the further reaction of $[Mo_7O_{23}(OH)]^{6-}$ in solution. The decomposition of $[Mo_7O_{23}(OH)]^{6-}$ can be also suggested by the decomposition of $[Mo_7O_{24}]^{6-}$ in the polarographic reduction.[20] In addition, a change in the pattern of the Raman spectrum after photolysis supports this possibility, as shown in Figure 5. From these results it is possible to say that the flash photolysis represents the decomposition process for $[Mo_7O_{23}(OH)]^{6-}$. The recent result that the blue species isolated from the photolyte consisted of two 'Keggin' structural 12- and 13-Mo atom molybdates (in a 2 : 1 ratio) [21] leads us to postulate the decondensation to 1-molybdate as the decomposition pathway for $[Mo_7O_{23}(OH)]^{6-}$. If reaction (10) is operative, the long-lived

$$[Mo_7O_{23}(OH)]^{6-} \longrightarrow \text{1-molybdate} \quad (10)$$

second species (II) with a lifetime of τ 10^2 s and $\lambda_{max.} = 500$ nm (in Figure 6) may be tentatively assigned to the one-electron reduced octahedral 1-molybdate (with $g = 1.910$), considering that 1-molybdate has a tendency to increase its co-ordination number from four to six at moderate concentration below pH 7.[22] Thus the first intermediate (I) with τ *ca.* 10^{-4} s may be assigned to the one-electron reduced 7- or 6-molybdate (with $g = 1.921$). At present, we cannot explain how 12- and 13-molybdates are formed as the blue species. The explanation at the molecular level must be left to further investigations.

[0/1071 *Received*, 7th *July*, 1980]

REFERENCES

[1] Part 4, T. Yamase, *J. Chem. Soc., Dalton Trans.*, 1978, 283.
[2] T. Yamase and T. Ikawa, *Inorg. Chim. Acta*, 1979, **37**, L529.
[3] T. Yamase and T. Ikawa, *Inorg. Chim. Acta*, 1980, **45**, L55.
[4] T. Yamase, T. Ikawa, H. Kokado, and E. Inoue, *Chem. Lett.*, 1973, 615; T. Yamase, H. Hayashi, and T. Ikawa, *ibid.*, 1974, 1055.
[5] T. Yamase and T. Ikawa, *Bull. Chem. Soc. Jpn.*, 1977, **50**, 746.
[6] K. Yanagi, Y. Ohashi, Y. Sasada, and T. Yamase, *Bull. Chem. Soc. Jpn.*, submitted for publication.
[7] E. G. Janzen, *Acc. Chem. Res.*, 1971, **4**, 31; T. Yamase, T. Ikawa, H. Kokado, and E. Inoue, *Photogr. Sci. Eng.*, 1974, **18**, 647.
[8] W. D. Emmons, *J. Am. Chem. Soc.*, 1957, **79**, 5739, 6522.
[9] C. A. Parker, *Proc. R. Soc. London, Ser. A*, 1953, **220**, 104.
[10] M. Pesez and J. Bartos, 'Colorimetric and Fluorimetric Analysis of Organic Compounds and Drugs,' Marcel Dekker, New York, 1974, p. 255.
[11] J.-P. Collin, P. Lagrange, and J.-P. Schwing, *J. Less-Common Met.*, 1974, **36**, 117, and references therein.
[12] M. Isobe, F. Marumo, T. Yamase, and T. Ikawa, *Acta Crystallogr.*, 1978, **B34**, 2728.
[13] E. G. Janzen, D. E. Nutter, E. R. Davis, B. J. Blackburn, J. L. Poyer, and P. B. McCay, *Can. J. Chem.*, 1978, **56**, 2337.
[14] W. P. Griffith and P. J. B. Lesniak, *J. Chem. Soc. A*, 1969, 1066; J. Aveston, E. W. Anacker, and J. S. Johnson, *Inorg. Chem.*, 1965, **3**, 735; R. H. Busey and O. L. Keller, *J. Chem. Phys.*, 1964, **41**, 215.

[15] H. T. Evans, B. M. Gatehouse, and P. Leverett, *J. Chem. Soc., Dalton Trans.*, 1975, 2728.
[16] D. Dobos, 'Electrochemical Data,' Marcel Dekker, New York, 1974.
[17] K. K. Barnes and C. K. Mann, *J. Org. Chem.*, 1967, **13**, 157.
[18] C. K. Mann, *Anal. Chem.*, 1964, **13**, 2424.
[19] I. Larking and R. Stomberg, *Acta Chem. Scand.*, 1972, **26**, 3708.
[20] G. P. Haight and D. R. Boston, *J. Less-Common Met.*, 1974, **36**, 95.
[21] T. Yamase, T. Ikawa, Y. Ohashi, and Y. Sasada, *J. Chem. Soc., Chem. Commun.*, 1979, 697.
[22] D. S. Honig and K. Kustin, *Inorg. Chem.*, 1972, **11**, 65; Y. Sasaki and A. G. Sykes, *J. Less-Common Met.*, 1974, **36**, 125.